NANODIAMOND LOADED FISH GELATIN ENZYMATICALLY CROSSLINKED HYDROGELS

Elena OLĂREȚ[1], Doris STEINMÜLLER-NETHL[2], Horia IOVU[3], Izabela-Cristina STANCU[4]

This study describes a green route for in-situ synthesis of gelatin-based hydrogels for biomedical applications. Scaffolds based on high protein content were obtained using 50% wt/vol and 70% (wt/vol) fish gelatin, as such or loaded with 1% wt/vol diamond nanoparticles. Transglutaminase was used as crosslinking agent and its network-forming efficiency was evaluated through gel fraction determination. The effects of both protein and nanoparticles were explored through swelling behavior and mechanical properties. Compressive modulus was found to be in range of 50-70 kPa while the storage modulus at surface in range of 1-9 kPa.

Keywords: fish gelatin, transglutaminase, enzymatic crosslinking, mechanical properties, diamond nanoparticles

1. Introduction

Over the years, hydrogels gain much attention in biomedical field being suitable for numerous applications among which many are commercially available: various types of wound dressing, intraocular lenses, drug delivery systems, etc. [1]. Hydrogels based on natural polymers have the advantage of high biocompatibility, but they are mechanically insufficient which often leads to development of hybrid or composite formulation when hard tissue is envisaged.

An interesting approach is represented by *in situ* forming hydrogels which find their main applications as injectable hydrogels - minimally invasive devices. These types of hydrogels can be obtained through both, physical and chemical crosslinking and usually they are found in a flow injectable state at room temperature and can suffer a sol-gel transition under different physiological conditions [2]. Beside all the characteristics advantages of hydrogels, this

[1] PhD student, Dept. of Bioresources and Polymer Science, Faculty of Applied Chemistry and Materials Science, Advanced Polymer Materials Group, University "POLITEHNICA" of Bucharest, Romania, e-mail: elena.olaret@upb.ro
[2] DiaCoating GmbH, 6112 Wattens, Austria; doris.steinmueller@diacoating.com
[3] Prof., Dept. of Bioresources and Polymer Science, Faculty of Applied Chemistry and Materials Science, Advanced Polymer Materials Group, University "POLITEHNICA" of Bucharest, Romania, e-mail: horia.iovu@upb.ro
[4] Prof., Dept. of Bioresources and Polymer Science, Faculty of Applied Chemistry and Materials Science, Advanced Polymer Materials Group and Faculty of Medical Engineering University "POLITEHNICA" of Bucharest, Romania, e-mail: izabela.stancu@upb.ro

particular type of *in-situ* network formation can result in complex shapes that are often encountered and hard to be filled. Ionic, hydrophobic and supramolecular interactions are the main strategies for physical crosslinked hydrogels while photo-crosslinking, click chemistry, Michael-type addition or Schiff base crosslinking can be found among the covalent crosslinking strategies [3]. However, one advantageous approach which provide reaction at physiological temperature and excellent biocompatibility is the biological crosslinking. Enzymes like transglutaminases, horseradish peroxidase or phosphatases are the most used for various type of hydrogels synthesis. Among them, transglutaminase (TGase) is the only one commercially available for food industry purposes [4]. TGases are a family of enzymes which in mammalian tissue are calcium-dependent and have important roles in regulating cell-matrix interactions [5–8]. On the other hand, microbial TGases are calcium independent and found applicability in a wide range of domains among which, food industry which takes full advantage of their binding properties [4,9,10].

TGase acts as a crosslinking agent through an acyl transfer reaction when ε-(γ-glutamyl)lysine isopeptide bonds are created between the carboxyamide group of glutamine residues and a primary amine from a lysine residue, for instance [9,10].

Fish gelatin (FG) is a well-known and widely used collagen derived biopolymer. There are many properties which recommend gelatin for biomedical applications among which the presence of RGD motif (known for its ability to mediate cell adhesion) [11]. Crosslinking of gelatin or collagen with TGase have been successfully done before to obtain films or hydrogels with applications in food or pharmaceutical industry [12–15]. Diamond nanoparticles (NDs) are remarkable carbon- based nanomaterials which due to their biocompatibility, unique surface structure, superior mechanical properties and chemical stability are wildly used in biomedical research area [16–19]. Our previous studies proved the biocompatibility of fish gelatin-diamond nanoparticles fibrous scaffolds crosslinked with glutaraldehyde [17–19], while biocompatibility of gelatin-TGase hydrogels in relation to adipose tissue-derived stromal cells [15], human embryonic kidney cell [20] has been reported by other groups. However, to the best of our knowledge, enzymatically crosslinked fish gelatin hydrogels loaded with diamond nanoparticles have not been reported yet.

This study aims to *in-situ* synthesize FG-NDs hydrogels by a friendly enzymatic crosslinking. Their structural characterization, swelling behavior and mechanical properties were investigated.

2. Materials and methods

2.1 Materials

Cold water fish skin gelatin (FG) was purchased from Sigma Aldrich. Carboxyl-functionalized diamond nanoparticles (NDs) were used as 1% (wt/v) aqueous dispersion (DiaCoating, Austria) and transglutaminase (TGase) with an enzymatic activity declared in range 80-120U/g (Transpower W, RAPS) was used as received, without further purification. Double distilled water was used for all compositions.

2.2 Methods

2.2.1 Hydrogels synthesis

Hydrogel precursors were prepared as described in table 1. Basically, the proper amount of FG was added to distilled water and 1% wt/vol NDs dispersion until a final concentration of 50% wt/vol and 70% wt/vol. Prior FG addition, 30 minutes sonication treatment was applied to NDs dispersion. FG was let to dissolve for four hours at 40°C. Then, proper amount of TGase was stepwise added while continuously stirring the precursors, for 30 minutes, at 4°C on an ice bath. The enzyme activity units/ gram of protein solution was maintained to 5U/g (considering an average TGase activity of 100U/g). The resulting viscous compositions were poured into molds (0.8 ml/well, using 24 wells cell culture plates) and kept at 37°C overnight, to allow enzymatic crosslinking to occur.

2.2.2 Hydrogels characterization

Crosslinking efficiency was determined by means of gel fraction investigation. Samples were dried at 37°C for 48 hours and weighted (m_0) immediately after crosslinking. Then, samples were immersed in distilled water at 37°C for 24 hours, dried and weighted again (m_f). Gel fraction (GF, %) was calculated according to equation 1.

$$\boldsymbol{GF}, \% = \frac{m_f}{m_0} \times 100 \quad (1)$$

Structural evaluation was performed through Fourier transform infrared with attenuated total reflectance (ATR-FTIR) measurements using a Jasco 4200 spectrometer equipped with a Specac Golden Gate ATR device, with a resolution of 4 cm^{-1}, in the wavenumber region of 4000–600 cm^{-1}.

Water affinity was investigated through conventional gravimetric method. Dried samples were weighted (m_i), immersed in distilled water and kept at 37°C. At different time points, the swollen samples were removed from incubation medium, the water excess was gently wiped with filter paper and the samples were weighted (m_t). Swelling degree (SD, %) of dried samples was computed according to equation 2.

$$\boldsymbol{SD}, \% = \frac{m_t - m_i}{m_i} \times \mathbf{100} \quad (2)$$

Maximum swelling degree (MSD, %) and equilibrium water content (EWC, %) were also determined gravimetrically. Samples were dried, weighted (m_{0MSD}) and fully immersed in water at 37°C. After 48 hours, samples were removed from water, blotted with filter paper and weighted again (m_{MSD}). MSD and EWC were computed according to equation 3 and equation 4 respectively.

$$\boldsymbol{MSD}, \% = \frac{m_{MSD} - m_{0MSD}}{m_{0MSD}} \text{ x } 100 \quad (3)$$

$$\boldsymbol{EWC}, \% = \frac{m_{MSD} - m_{0MSD}}{m_{MSD}} \text{ x } 100 \quad (4)$$

Swelling kinetics were investigated in respect to equation 5, as described in [21]:

$$\boldsymbol{f} = \frac{w_t}{w_\infty} = \boldsymbol{kt^n} \quad (5)$$

where "f" expresses the swelling fraction and it is equal to the ratio between the weight of water within hydrogel at time t (w_t) and weight of water within hydrogel when equilibrium is reached (w_∞); "k" represents a constant characteristic to the hydrogel structure, "t" is the swelling time and "n" is a number that indicates which swelling mechanism (Fickian or non-Fickian diffusion) controls the water uptake of the tested hydrogel. Equation 5 is valid only for the first 60% fractional water uptake.

Mechanical properties of hydrogels were evaluated through uniaxial compression and through indentation tests. Fully swollen cylindrical hydrogels, with a radius of 4 mm and a thickness of 2 mm were used for both types of determinations. *Mechanical properties through uniaxial compression* were studied using a Brookfield CT3 texture analyzer at room temperature. Samples were fixed on a bottom plate and perpendicularly compressed by the upper platen connected to a 45N load cell with a test speed of 0.5 mm/s. Compression modulus was computed as the slope of the linear zone of stress-strain curves at 1% strain.
Indentation tests were performed using a Nano Indenter ® G200 system configured with a DCM head and a continuous stiffness measurement option (CSM). A DCM II diamond flat-punch indenter tip with radius of 50 µm was used. Storage modulus (G') and loss modulus (G') were determined according to "G-Series DCM CSM Flat Punch Complex Modulus, Gel" NanoSuite method. Four different indentations separated by at least 500 µm were performed on each sample. The testing frequency was set to 10 Hz.

All experiments were performed minimum in triplicate (n=3) and statistical significance was evaluated using one-way ANOVA method. Differences were considered statistically significant for $p < 0.05$. NS - no statistically significant, *p<0.05, **p<0.01, ***p<0.001

3. Results and discussion

Hydrogels with high protein content, loaded with nanospecies, where *in-situ* synthetized by adapting the protocol from RO132544B1 [22]. Fig. 1 shows the schematic representation of preparative steps. Dissolution of FG takes place at 40°C in NDs suspension or in distilled water; in addition to FG-FG intermolecular interactions, physical interactions such as H-bonding between functional groups of FG macromolecules and NDs are expected in the nanostructured compositions (step 1 in Fig. 1).

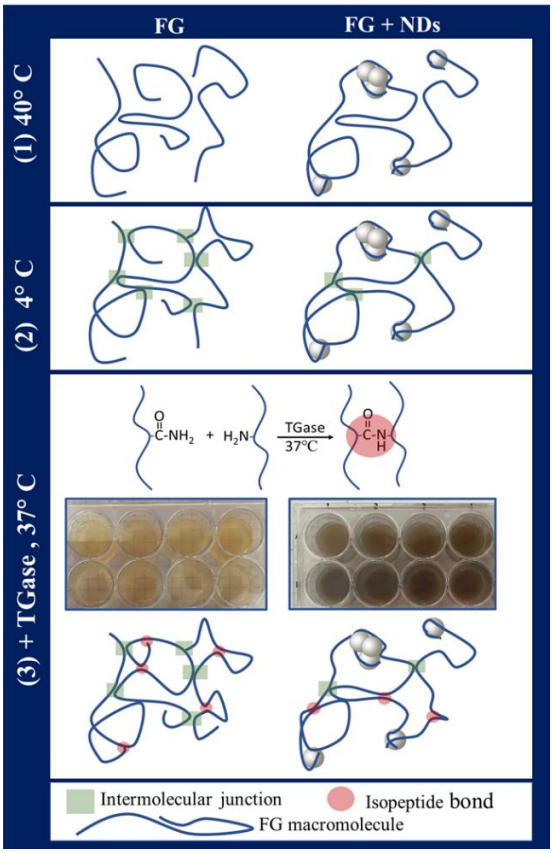

Fig. 1. Schematic representation of network forming mechanism in FG and FG-NDs hydrogels

To allow homogeneous distribution of the enzyme in the FG-based precursors, considering that TGase is thermally activated to induce protein crosslinking, the compositions are cooled to 4°C to prevent local reaction. The enzyme is added and the continuous stirring at 4°C is maintained for 30 minutes. Cooling is associated with molecular rearrangements of FG macromolecules favoring helical conformation due to more intense H bonds and junction zones (step 2 in Fig. 1), followed by shrinkage of the physically formed network [23].

FG-NDs interactions are also present in the corresponding samples (step 2 in Fig. 1). Then, the precursors are poured into molds and the crosslinking is initiated by heating at 37°C. This stimulates FG unfolding simultaneously with the isopeptide bonds formation following TGase crosslinking (step 3 in Fig. 1). Subsequent the overnight incubation at 37°C, hydrated elastic insoluble networks are formed.

Gel fraction. To study the efficiency of network formation, gel fraction (GF) evaluation was performed. Through this investigation, uncrosslinked protein soluble fraction may be removed by extraction in distilled water, at 37°C. The values obtained for GF were gravimetrically determined according to equation 1 and are listed in Table 1. Considering that TGase: FG ratio was kept constant, all differences in GF can be assigned to nanoparticles presence or to the different protein content used. Results showed that both, the presence of NDs and the FG concentration, have a significant influence on GF. While NDs presence led to lower GF values, increasing the protein content improves the GF. The effect of NDs suggests that the low reduction in crosslinking efficiency (about 3%) is probably due to a suppression of protein segmental mobility and hindering of protein-enzyme interactions due to the nanoparticles. Similar effect of NDs on protein mobility were reported in a previous work when FG at similar protein contents was crosslinked with glutaraldehyde [17].

Table 1

Crosslinking efficiency as function of composition (mean ± standard deviation, n=3)

Sample name	NDs: FG wt/wt ratio	FG concentration wt/vol	Gel fraction, %	p value		
FG50	-	50 %	83.85 ± 0.4	0.008	0.0004	
FG50_NDs	2 %		80.93 ± 0.8			0.0006
FG70	-	70 %	88.44 ± 0.8	0.004		
FG70_NDs	1.4 %		85.27 ± 0.7			

Structural characterization through FTIR spectroscopy was performed on the obtained hydrogels and on the raw materials (Fig. 2). FG spectrum shows characteristics broad and intense peaks at 3276 cm^{-1} assigned to amide A with contribution form OH and H bonds. Amide B is noticed at 3075 cm^{-1}. This is in agreement with other studies [24][25]. Amide A signal was shifted to 3295 cm^{-1} for both FG50 and FG70, to 3294 cm^{-1} for FG50_NDs and to 3278 for FG70_NDs. Usually, free N-H stretching vibration may vary between 3440-3400 cm^{-1} [26] while shifts to lower wavenumbers typically suggest engagement in H bonds [27]. Increasing FG to 70% in FG70_NDs seems to attenuate the effect of nanoparticles and crosslinking. The nanocomposite samples recorded a red shift for amide B (3057 and 3051 cm^{-1}) as well, most probably due to decreasing number of $-NH_3^+$ and NH_2 groups through isopeptide bond formation [26–28]. Amide I which is attributed to stretching vibration of C=O, presented a strong peak at 1632 cm^{-1} in FG spectrum and at similar wavenumbers for FG50 (1634

cm^{-1}) and FG50_NDs (1631 cm^{-1}). These values are typically associated with β-sheet-rich protein structures [29].

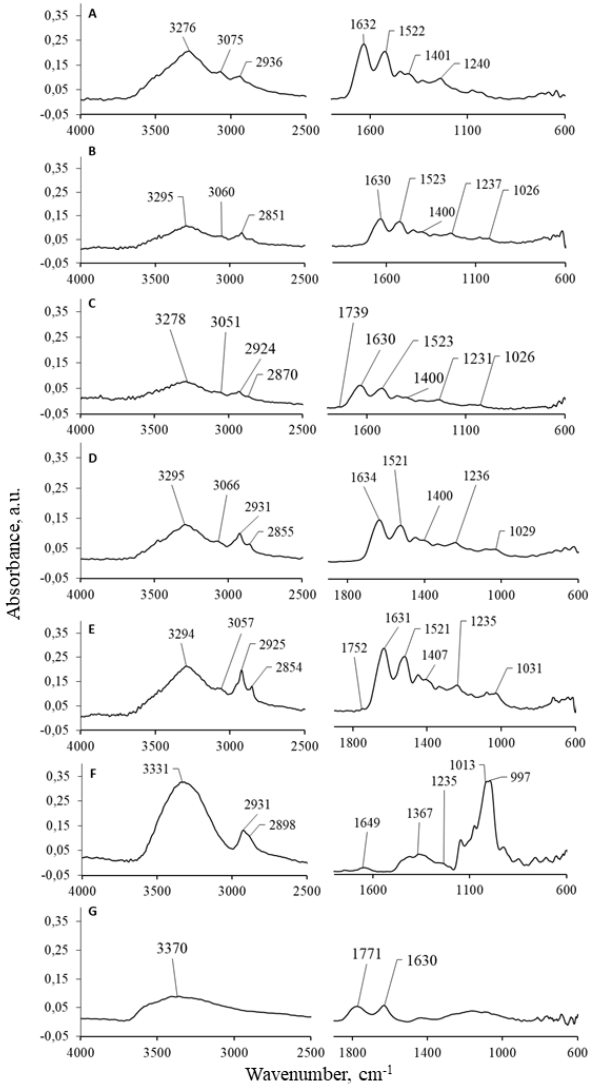

Fig. 2. Representative ATR-FTIR spectra: A. FG, B. FG70, C. FG70_NDs, D. FG50, E. FG70_NDs, F. TGase and G. NDs-COOH

Amide I and II vibrations also suggest secondary structure modifications due to H-bonding microenvironments [30]. Amide II, related to C-N stretch and CNH deformation vibrations, showed peaks at 1521 cm^{-1} for FG50-based samples and at 1523 cm^{-1} for FG70-based samples. Interestingly, the effect of NDs is not detected while the protein amount seems to impose the amide II value. Amide III, assigned to C-N stretch, N-H bend and CO in-plane bend, were recorded at 1240

cm^{-1}, 1236 cm^{-1} and 1235 cm^{-1} for FG, FG50 hydrogel and FG50_NDs nanocomposite, while in FG70 and FG70_NDs they appear at 1237 cm^{-1} and 1231 cm^{-1}. NDs spectrum recorded a specific C=O stretching vibration (from carboxylic groups) at 1771 cm^{-1} and of other origin (ketone) at 1630 cm^{-1} [19]. Probably due to the low amount of NDs in hydrogels, their specific bands appear only as small peaks at 1752 cm^{-1} in FG50_NDs spectrum and at 1739 cm^{-1} in FG70_NDs. Additionally, all samples recorded an absorption peak around 1026 – 1031 cm^{-1} which can be correlated to the presence of maltodextrin (alimentary additive) in commercial TGase [25,31]. Absorption band related to vibration of C-H bonds found in between 2925 cm^{-1} and 2936 cm^{-1} increased in intensity in TGase treated samples [31].

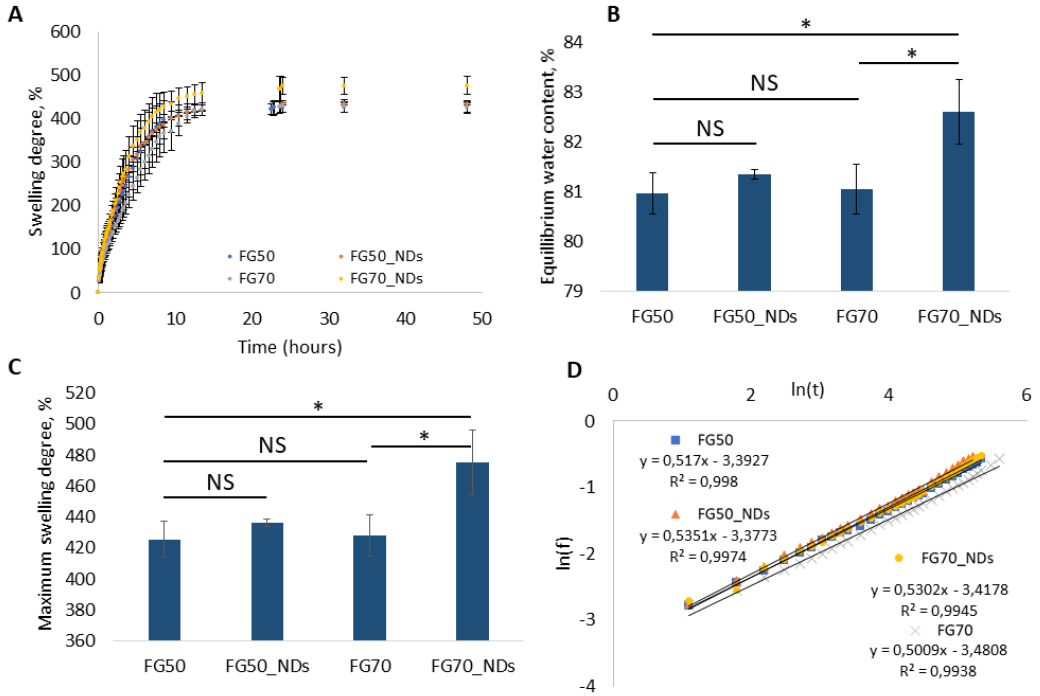

Fig. 3. Swelling behavior of hydrogels during 48h in distilled water at 37°C, (A) % swelling degree, (B) equilibrium water content, (C) maximum swelling degree, (D) swelling kinetics expressed in ln(f) as function of ln(t); (n=3, mean ± standard deviation, *p<0.05);

Swelling behavior was monitored for 48h at 37°C in distilled water. As it can be observed in Fig. 3A, all samples reached equilibrium (MSD) within 24 hours, with a fast hydration in the first 10 hours, followed by a slower water retention. While FG50 and FG70 behave similarly, the swelling capacity was slightly increased for FG50_NDs and significantly improved for FG70_NDs which recorded the highest MSD and EWC (Fig. 3B,C). Due to H-bonds that might occur between NDs and FG before the addition of TGase, nanoparticles

presence could act as a loosener of crosslinking density, hence higher swelling capacity is recorded for NDs loaded hydrogels. This result is different when compared to swelling enhancement by NDs in FG70_NDs electrospun microfibers crosslinked with glutaraldehyde (GA) vapors [17]. This suggests the importance of both the geometry of scaffolds (hydrated block versus fibrous) and of the crosslinking mechanism (bulk for the in situ-enzyme exposure versus diffusion based for GA).

Water transport within a hydrogel depends on many factors among which, chemical composition, crosslinking density, equilibrium water content etc. Water transport can be divided in Fickian diffusion and non-Fickian diffusion [21]. Fickian diffusion, known also as Case I, takes place when water diffusion rate is slower than polymer chain relaxation rate. Contrary, non-Fickian diffusion, known as Case II, takes place when water diffusion rate is faster than polymer chain relaxation rate [21][32]. In between these 2 types of diffusion, anomalous diffusion, also a non-Fickian mechanism takes place when both, water diffusion and polymer chain relaxation rates have roughly the same value.

Fig. 3.D shows ln(f) *versus* ln(t) plots as obtained after applying natural logarithm to equation 4. The swelling mechanism is given by the slope of these plots (n parameter) while the intercept expresses the ln(k). Fickian diffusion and Case II mechanisms are described by n values of 0.5 and 1 respectively, while values of n between 0.5 and 1 suggest non-Fickian transport mechanism (relaxation controlled)[33]. Water transport mechanism was defined by values of n close to 0.5. Kinetic parameters are presented in Table 2.

Table 2

Water transport kinetic parameters, 37°C

Sample	n	k *100	R^2
FG50	0.52	3.36	0.998
FG50_NDs	0.54	3.41	0.9974
FG70	0.50	3.08	0.9938
FG70_NDs	0.53	3.28	0.9945

Mechanical properties of the *in-situ* crosslinked hydrogels were evaluated through compression and indentation test. All tests were performed at room temperature after fully hydrated at 37°C in PBS. Compressive modulus (E) was calculated from the slope of the linear zone of stress-strain curves at 1% strain. Fig. 4 shows the graphical representation of the obtained data. Both, protein increase and addition of NDs, reinforce the hydrated scaffolds (Fig. 4A,B). The nanostructuring effect of NDs is stronger for FG50 than for FG70. When compared to water affinity data, it results that the elasticity is not mainly swelling-controlled, but the mechanical properties of NDs play an important role as well.

When considering biomedical applications mechanical properties at surface are of great interest [34]. Therefore, indentation tests were performed on

hydrated samples. An indentation test takes around 4 minutes to be complete and it returns G' and G'' which are calculated according to equation 5 and equation 6, where S is the contact stiffness, ν is Poisson's ratio and is set to 0.5, D is the punch diameter and Cω is the contact damping [35–37].

$$G' = S(1-\nu)/(2D) \quad (5)$$

$$G'' = C\omega(1-\nu)/(2D) \quad (6)$$

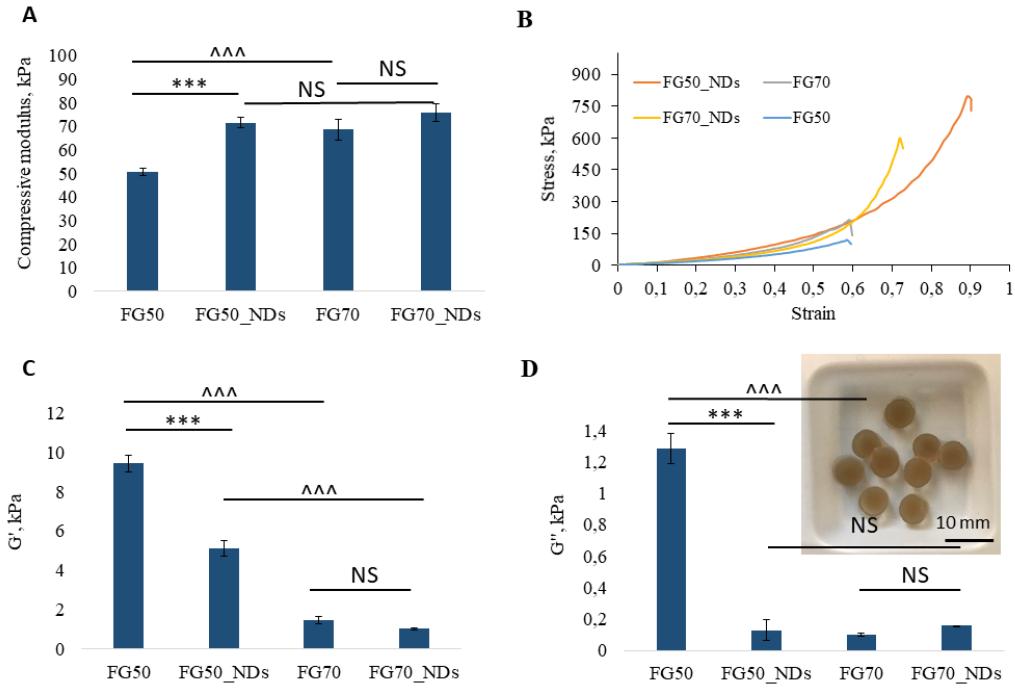

Fig. 4. Mechanical properties obtained using a texture analyzer (A,B) and a nanoindenter (C,D): (A) Compressive modulus calculated at 1% strain (n=3, mean ± standard deviation, NS), (B) Representative stress-deformation curves for each composition, (C) Storage modulus (G') and , (D) Loss modulus (G") as obtained from nanoindentation test conducted at 10 Hz testing frequency and 5 µm indentation depth; (n=4, mean ± standard deviation, ***p<0.001, ^^^p<0.001); (D) inset: digital image with NDs loaded samples used for mechanical testing

G', known as storage modulus or elasticity modulus give information about the elastic behavior (hydrogel ability to store energy) while G", known as loss modulus or viscosity modulus give information about the viscous behavior (or hydrogel ability to dissipate energy) [38]. For all samples the elastic behavior is stronger than viscous behavior, as expected considering the hydrogel matrix (Fig. C,D). As it can be observed in Fig. 4C, the mechanical properties at surface are weaker when compared to bulk mechanical properties obtained under uniaxial compression (Fig. 4A). Furthermore, surface mechanical properties of FG70 and FG70_NDs were found to be in range of ultrasoft tissue such as brain tissue

[39][40] while FG50 and FG50_NDs falls in soft tissue range, such as human skin [41].

Table 3

Mechanical properties correlated with equilibrium water content of hydrogels

Sample	E (kPa)	G' (kPa)	G" (kPa)	EWC, %
FG50	50,54 ± 1,52	9.43 ± 0.42	1.29 ± 0.09	80.97 ± 0.41
FG50_NDs	71,61 ± 2,03	5.10 ± 0.4	0.13 ± 0.07	81.35 ± 0.09
FG70	68,65 ± 4,38	1.46 ± 0.2	0.10 ± 0.01	81.05 ± 0.5
FG70_NDs	75,79 ±3,94	1.01 ±0.05	0.16 ± 0.00	82.60 ± 0.64

4. Conclusion

Nanocomposite hydrogels based on FG and NDs were *in-situ* synthesized at physiological temperature through an enzymatic crosslinking. The crosslinking efficiency of TGase was found to be higher for samples with higher protein content. All samples showed high swelling capacity characterized by a non-Fickian water transport mechanism apart from FG70. Moreover, presence of NDs, even in such low loading significantly influence the crosslinking efficiency. Swelling behavior and mechanical properties were also influenced by NDs addition. We believe that NDs interacts with the reactive groups before crosslinking and acts as a spacer within the polymeric network after rehydration, however, interactions between FG and NDs will be further investigated. These preliminary results suggest the potential of FG-NDs hydrogels as materials for soft tissue engineering.

The developed formulation is suitable for in situ enzymatic crosslinking further allowing the use of these compositions as fillers for complex-shaped defects. Furthermore, the potential of such biomaterials to be used as a bio-glue will be investigated, considering the ability of TGase to also crosslink collagen from the walls of the tissue defect. Moreover, the presence of NDs, will be further tackled for the possibility to be exploited as drug delivery or growth factor nanoplatforms.

Acknowledgement

The nanoindentation tests were possible due to European Regional Development Fund through Competitiveness Operational Program 2014–2020, Priority axis 1, Project No. P_36_611, MySMIS code 107066, Innovative Technologies for Materials Quality Assurance in Health, Energy and Environmental—Center for Innovative Manufacturing Solutions of Smart Biomaterials and Biomedical Surfaces—INOVABIOMED.

R E F E R E N C E S

[1] *S.H. Aswathy, U. Narendrakumar, I. Manjubala*, "Commercial hydrogels for biomedical applications", Heliyon., **vol. 6**, no.4, 2020, p.e03719.

[2] *R. Dimatteo, N.J. Darling, T. Segura*, „In situ forming injectable hydrogels for drug delivery and wound repair", Adv. Drug Deliv. Rev., **vol. 127**, 2018, pp.167–184.

[3] *F. Poustchi, H. Amani, Z. Ahmadian, S.V. Niknezhad, S. Mehrabi, H.A. Santos, M. Shahbazi*, „Combination Therapy of Killing Diseases by Injectable Hydrogels: From Concept to Medical Applications", Adv. Healthc. Mater., **vol. 10**, no.3, 2021, p.2001571.

[4] *S. Isaschar-Ovdat, A. Fishman*, „Crosslinking of food proteins mediated by oxidative enzymes – A review", Trends Food Sci. Technol., **vol. 72**, 2018, pp.134–143.

[5] *C. Klöck, C. Khosla*, "Regulation of the activities of the mammalian transglutaminase family of enzymes", Protein Sci., **vol. 21**, 2012, pp. 1781–1791.

[6] *L. Fesus, M. Piacentini*, „Transglutaminase 2: an enigmatic enzyme with diverse functions", Trends Biochem. Sci., **vol. 27**, 2002, pp.534–539.

[7] *A. Zemskov, Evgeny*, „The role of tissue transglutaminase in cell-matrix interactions", Front. Biosci, **vol. 11**, 2006, p.1057.

[8] *A. Di Sabatino, A. Vanoli, P. Giuffrida, O. Luinetti, E. Solcia, G.R. Corazza*, „The function of tissue transglutaminase in celiac disease", Autoimmun. Rev., **vol. 11**, 2012, pp.746–753.

[9] *H.S. Mostafa*, „Microbial transglutaminase: An overview of recent applications in food and packaging", Biocatal. Biotransformation., **vol. 38,** 2020, pp.161–177.

[10] *M. Kieliszek, A. Misiewicz*, „Microbial transglutaminase and its application in the food industry. A review", Folia Microbiol. (Praha)., **vol. 59,** 2014, pp.241–250.

[11] *L.-C. Lv, Q.-Y. Huang, W. Ding, X.-H. Xiao, H.-Y. Zhang, L.-X. Xiong*, „Fish gelatin: The novel potential applications", J. Funct. Foods., **vol. 63,** 2019, p.103581.

[12] *H. Rostamzad, S.Y. Paighambari, B. Shabanpour, S.M. Ojagh, S.M. Mousavi*, „Improvement of fish protein film with nanoclay and transglutaminase for food packaging", Food Packag. Shelf Life., **vol. 7,** 2016, pp. 1–7.

[13] *Y. Garcia, R. Collighan, M. Griffin, A. Pandit*, „Assessment of cell viability in a three-dimensional enzymatically cross-linked collagen scaffold", J. Mater. Sci. Mater. Med., **vol. 18,** 2007, pp.1991–2001.

[14] *Z.Y. Liu, Y. Lu, X.J. Ge, M.Y. Zeng*, „Effects of Transglutaminase on Rheological and Film Forming Properties of Fish Gelatin", Adv. Mater. Res., **vol. 236–238,** 2011, pp.2877–2880.

[15] *G. Yang, Z. Xiao, X. Ren, H. Long, H. Qian, K. Ma, Y. Guo*, „Enzymatically crosslinked gelatin hydrogel promotes the proliferation of adipose tissue-derived stromal cells", PeerJ., **vol. 4**, 2016, p.e2497.

[16] *C.Ş. Iosub, E. Olăreț, A.M. Grumezescu, A.M. Holban, E. Andronescu*, „Toxicity of nanostructures—a general approach", Nanostructures Nov. Ther., Elsevier, 2017: pp. 793–809.

[17] *E. Olăreț, D.-M. Drăguşin, A. Serafim, A. Lungu, A. Şelaru, A. Dobranici, S. Dinescu, M. Costache, I. Boerașu, B. Ștefan Vasile, D. Steinmüller-Nethl, H. Iovu, I.-C. Stancu*, „Electrospinning Fabrication and Cytocompatibility Investigation of Nanodiamond Particles-Gelatin Fibrous Tubular Scaffolds for Nerve Regeneration", Polymers, **vol. 13,** 2021, p.407

[18] *A. Serafim, S. Cecoltan, A. Lungu, E. Vasile, H. Iovu, I.C. Stancu*, „Electrospun fish gelatin fibrous scaffolds with improved bio-interactions due to carboxylated nanodiamond loading", RSC Adv., **vol. 5**, 2015 pp.95467–95477.

[19] *A. Şelaru, D.-M. Drăguşin, E. Olăreț, A. Serafim, D. Steinmüller-Nethl, E. Vasile, H. Iovu, I.-C. Stancu, M. Costache, S. Dinescu*, „Fabrication and Biocompatibility Evaluation of Nanodiamonds-Gelatin Electrospun Materials Designed for Prospective Tissue Regeneration Applications", Materials., **vol.12,** 2019, p.2933.

[20] *C.W. Yung, L.Q. Wu, J.A. Tullman, G.F. Payne, W.E. Bentley, T.A. Barbari*, „Transglutaminase crosslinked gelatin as a tissue engineering scaffold", J. Biomed. Mater. Res. Part A., **vol. 83A**, no.4, 2007, pp.1039–1046.

[21] J. *Ostrowska-Czubenko, M. Gierszewska, M. Pieróg*, „pH-responsive hydrogel membranes based on modified chitosan: water transport and kinetics of swelling", J. Polym. Res., **vol. 22**, 2015, p.153.
[22] *I.-C. Stancu, S. Cecoltan, D. G. Petre, A. Lungu, A. Serafim, D.-M. Draguşin, E. Vasile, R. Marinescu, A. Salageanu, C. Tucureanu, I. Caras, V.-C. Tofan, M. Istodorescu*, „Process for preparing bionanocomposite hydrated substrates for cell growth and tissue regeneration/modelling", RO132544B1, 2020.
[23] *M. Anvari, D. Chung*, „Effect of cooling–heating rate on sol-gel transformation of fish gelatin–gum arabic complex coacervate phase", Int. J. Biol. Macromol., **vol.91**, 2016, pp. 450–456.
[24] *F. Casanova, M.A. Mohammadifar, M. Jahromi, H.O. Petersen, J.J. Sloth, K.L. Eybye, S. Kobbelgaard, G. Jakobsen, F. Jessen*, „Physico-chemical, structural and techno-functional properties of gelatin from saithe (Pollachius virens) skin", Int. J. Biol. Macromol., **vol 156**, 2020, pp.918–927.
[25] *H. Staroszczyk, J. Pielichowska, K. Sztuka, J. Stangret, I. Kołodziejska*, "Molecular and structural characteristics of cod gelatin films modified with EDC and TGase", Food Chem., **vol. 130**, 2012, pp.335–343.
[26] *M.E.O. Martins, J.R. Sousa, R.L. Claudino, S.C.O. Lino, D.A. do Vale, A.L.C. Silva, J.P.S. Morais, M. de S.M. De Souza Filho, B.W.S. De Souza*, „Thermal and Chemical Properties of Gelatin from Tilapia (Oreochromis niloticus) Scale", J. Aquat. Food Prod. Technol., **vol. 27,** 2018, pp.1120–1133.
[27] *M. Ahmad, S. Benjakul*, „Characteristics of gelatin from the skin of unicorn leatherjacket (Aluterus monoceros) as influenced by acid pretreatment and extraction time", Food Hydrocoll., **vol.25**, 2011, pp.381–388.
[28] *P. Kaewprachu, K. Osako, W. Tongdeesoontorn, S. Rawdkuen*, „The effects of microbial transglutaminase on the properties of fish myofibrillar protein film", Food Packag. Shelf Life., **vol. 12**, 2017, pp.91–99.
[29] *P.I. Haris*, „Probing protein–protein interaction in biomembranes using Fourier transform infrared spectroscopy", Biochim. Biophys. Acta - Biomembr., **vol. 1828,** 2013, pp.2265–2271.
[30] *Á.I. López-Lorente, B. Mizaikoff*, „Mid-infrared spectroscopy for protein analysis: potential and challenges", Anal. Bioanal. Chem., **vol. 408**, 2016, pp.2875–2889.
[31] *E. Sritham, S. Gunasekaran*, „FTIR spectroscopic evaluation of sucrose-maltodextrin-sodium citrate bioglass", Food Hydrocoll., **vol. 70**, 2017, pp.371–382.
[32] *P.L. Ritger, N.A. Peppas*, „A simple equation for description of solute release II. Fickian and anomalous release from swellable devices", J. Control. Release., **vol. 5**, 1987, pp.37–42.
[33] *R.W. Korsmeyer, R. Gurny, E. Doelker, P. Buri, N.A.* "Peppas, Mechanisms of solute release from porous hydrophilic polymers", Int. J. Pharm., **vol.15**, 1983, pp.25–35.
[34] *J. Zonderland, L. Moroni*, „Steering cell behavior through mechanobiology in 3D: A regenerative medicine perspective", Biomaterials., **vol. 268**, 2021, p.120572.
[35] *I.N. Sneddon*, „The relation between load and penetration in the axisymmetric boussinesq problem for a punch of arbitrary profile", Int. J. Eng. Sci., **vol. 3**, 1965, pp.47–57.
[36] *E.G. Herbert, W.C. Oliver, A. Lumsdaine, G.M. Pharr*, „Measuring the constitutive behavior of viscoelastic solids in the time and frequency domain using flat punch nanoindentation", J. Mater. Res., **vol. 24**, 2009, pp.626–637.
[37] *E.G. Herbert, W.C. Oliver, G.M. Pharr*, „Nanoindentation and the dynamic characterization of viscoelastic solids", J. Phys. D. Appl. Phys., **vol. 41**, 2008, p.074021.
[38] *R. Moreno,"* Rheology", Encycl. Mater. Sci. Technol., Elsevier, 2001: pp. 8192–8196.

[39] *D.B. MacManus, B. Pierrat, J.G. Murphy, M.D. Gilchrist*, „Dynamic mechanical properties of murine brain tissue using micro-indentation", J. Biomech., **vol. 48**, 2015, pp.3213–3218.
[40] *S. Budday, R. Nay, R. de Rooij, P. Steinmann, T. Wyrobek, T.C. Ovaert, E. Kuhl*, „Mechanical properties of gray and white matter brain tissue by indentation", J. Mech. Behav. Biomed. Mater., **vol. 46**, 2015, pp.318–330.
[41] *G. Boyer, L. Laquièze, A. Le Bot, S. Laquièze, H. Zahouani*, „Dynamic indentation on human skin in vivo: ageing effects", Ski. Res. Technol., **vol. 15**, 2009, pp.55–67.